

ARTICLE



# Genetic differentiation and evolution of broad-leaved evergreen shrub and tree varieties of *Daphniphyllum macropodum* (Daphniphyllaceae)

Watanabe Yoichi<sup>1</sup>✉, Sae Matsuzawa<sup>2</sup>, Ichiro Tamaki<sup>3</sup>, Atsushi J. Nagano<sup>4,5</sup> and Sang-Hun Oh<sup>6</sup>

© The Author(s), under exclusive licence to The Genetics Society 2023

Tree form evolution is an important ecological specialization for woody species, but its evolutionary process with adaptation is poorly understood, especially on the microevolutionary scale. *Daphniphyllum macropodum* comprises two varieties: a tree variety growing in a warm temperate climate with light snowfall and a shrub variety growing in a cool temperate climate with heavy snowfall in Japan. Chloroplast DNA variations and genome-wide single-nucleotide polymorphisms across *D. macropodum* populations and *D. teijsmannii* as an outgroup were used to reveal the evolutionary process of the shrub variety. Population genetic analysis indicated that the two varieties diverged but were weakly differentiated. Approximate Bayesian computation analysis supported a scenario that assumed migration between the tree variety and the southern populations of the shrub variety. We found migration between the two varieties where the distributions of the two varieties are in contact, and it is concordant with higher tree height in the southern populations of the shrub variety than the northern populations. The genetic divergence between the two varieties was associated with snowfall. The heavy snowfall climate is considered to have developed since the middle Quaternary in this region. The estimated divergence time between the two varieties suggests that the evolution of the two varieties may be concordant with such paleoclimatic change.

*Heredity* (2023) 131:211–220; <https://doi.org/10.1038/s41437-023-00637-2>

## INTRODUCTION

Ecological specialization with adaptation, which is a genetic and evolutionary process increasing the fitness of a population to its environment, is commonly found in nature (Futuyma and Moreno 1988; Brown 1995). Studies on the evolutionary process and genome-wide differentiation associated with ecological differences contribute to understanding processes and mechanisms of ecological specialization (Hoekstra et al. 2006). From dwarf shrubs to canopy trees, the tree form is an important ecological specialization, such as competing with other species or individuals, reproducing effectively, and using limited resources (King 1990; Petit and Hampe 2006). Although this morphology is also influenced by the local environment, such as drought and wind stresses, the tree form is determined by hormone concentration of auxin and genetically predetermined for each species (Hollender and Dardick 2015); therefore, understanding tree form differences and its evolution contributes to forestry and other agriculture. Tree form variation is found in various taxa and within genera such as *Echium* (Böhle et al. 1996), *Lupinus* (Hughes and Eastwood 2006), and *Salix* (Wagner et al. 2018). Phylogenetic analyses revealed that tree form evolution occurred multiple times within a genus (Wagner et al. 2018). However, it is difficult to detect the genetic mechanism of tree form evolution from inter-specific

relationships because of excessive genetic divergence. The variation within species is limited, such as *Eucalyptus globulus* (Foster et al. 2007), and the evolutionary process within species can provide important knowledge for the ecological specialization of trees. In the case of *E. globulus*, shrub populations evolved in parallel in disjunct areas, suggesting that these populations were formed by environmental pressure or genetic mechanisms.

Generally, the growth of evergreen broad-leaved trees is restricted in cold areas because of the less cold hardiness of evergreen leaves (Sakai and Larcher 1987; Kume and Ino 1993). However, evergreen broad-leaved shrubs are characteristically distributed in a heavy snowfall region along the Sea of Japan of the Japanese archipelago (Maekawa 1949; Hara 2023), and it is considered that the distribution of the shrubs is enabled by protection in snow cover (Kume and Ino 1993). For example, evergreen broad-leaved shrubs such as *Camellia rusticana* (Theaceae), *Aucuba japonica* var. *borealis* (Garryaceae), *Ilex crenata* var. *paludosa*, *I. leucoclada* (Araliaceae), and *Daphniphyllum macropodum* var. *humile* (Daphniphyllaceae) are distributed in this heavy snowfall region. Interestingly, their tree or tall shrub congeners are distributed in a region along the Pacific Ocean with light snowfall, such as *C. japonica*, *A. japonica* var. *japonica*, *I. crenata* var. *crenata*, *I. integra*, and *D. macropodum* var.

<sup>1</sup>Graduate School of Horticulture, Chiba University, 648 Matsudo, Matsudo, Chiba 271-8510, Japan. <sup>2</sup>Faculty of Horticulture, Chiba University, 648 Matsudo, Matsudo, Chiba 271-8510, Japan. <sup>3</sup>Gifu Academy of Forest Science and Culture, 88 Sodai, Mino, Gifu, Japan. <sup>4</sup>Faculty of Agriculture, Ryukoku University, 1-5 Yokotani, Seta Oe-cho, Otsu, Shiga 520-2194, Japan. <sup>5</sup>Institute for Advanced Biosciences, Keio University, 403-1 Nipponkoku, Daishouji, Tsuruoka, Yamagata 997-0017, Japan. <sup>6</sup>Department of Biology, Daejeon University, 62 Daehak-ro, Dong-gu, Daejeon 34520, South Korea. Associate Editor: Pär Ingvarsson. ✉email: yoichi@nagoya-u.jp

Received: 12 March 2023 Revised: 16 June 2023 Accepted: 23 June 2023  
Published online: 17 July 2023

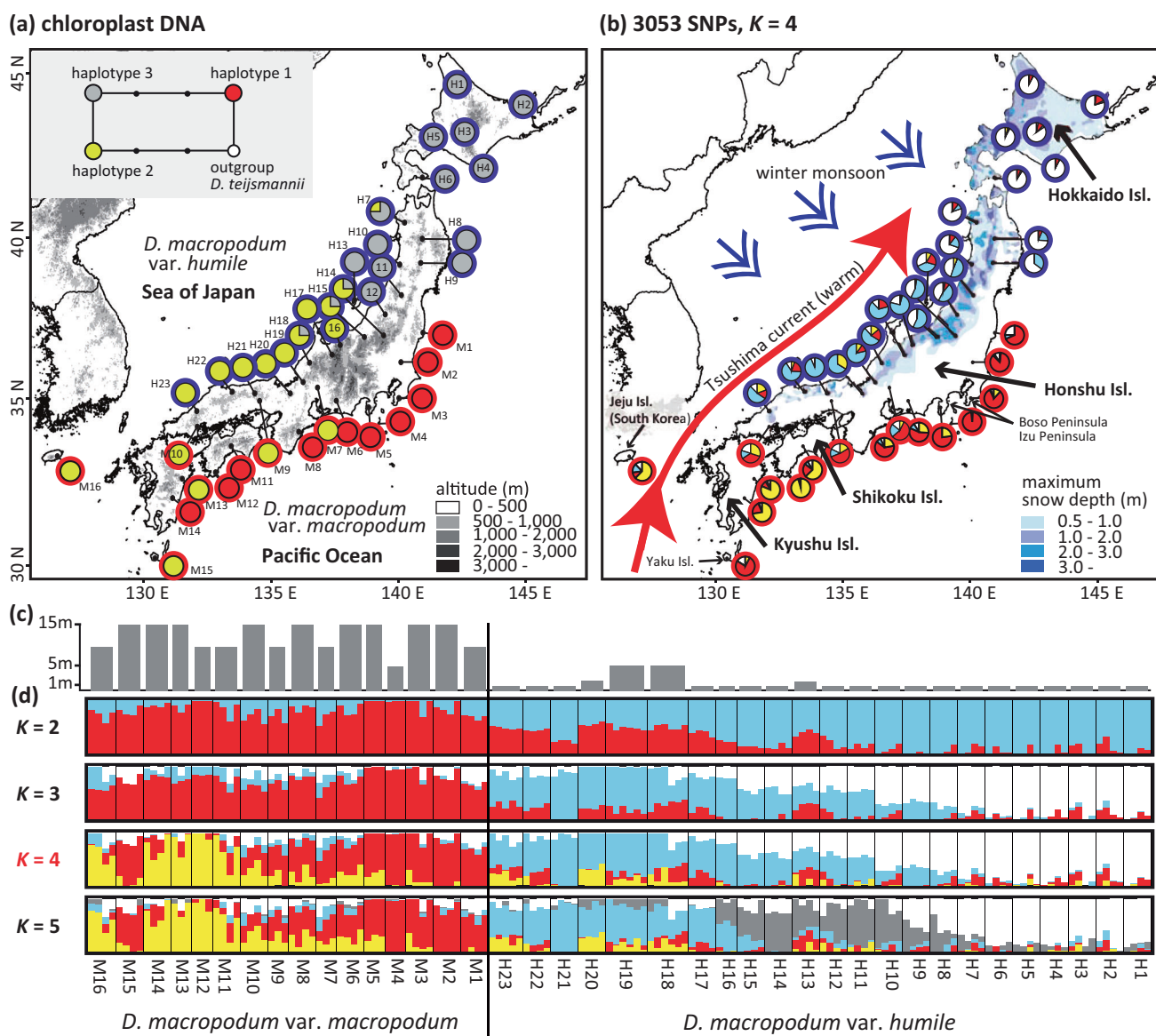


**Fig. 1 Distributions of analyzed populations and chloroplast DNA haplotypes, genetic clusters elucidated by sNMF, and approximate maximum tree height of the population.** **a** Small letters indicate population codes corresponding to those in Table 1. Pie charts indicate frequencies of chloroplast DNA haplotypes, and the green and blue outer circles of the pie charts indicate *Daphniphyllum macropodium* var. *macropodium* and var. *humile*, respectively. A haplotype network is superimposed on the map. **b** Geographical distributions of ancestry for the two varieties when  $K = 4$ , the optimal number of clusters supported by the cross-entropy criterion. Snow depth is shown only for Japan, which is modified data from Japan Meteorological Agency (<https://www.data.jma.go.jp/obd/stats/etrn/view/atlas.html>). **c** Approximate maximum tree height of the population. **d** Distributions of ancestry when the number of clusters ranged from  $K = 2$ –5.

*macropodium* (Maekawa 1949; Hara 2023). The maximum snow depth in the Japanese archipelago along the Sea of Japan is sometimes over than 4 m (Fig. 1). It is caused by three factors: the cold winter monsoon from the northwest, the warm Tsushima current in the Sea of Japan, and continuous mountain ranges along the Sea of Japan (Kawase et al. 2018). Clouds are formed by contact between the cold air and warm current and move to the Japanese mountains during strong winter monsoons, resulting in heavy snowfall in the mountains. Global cooling started in the mid-Miocene and climatic oscillations started in the Pleistocene (Zachos et al. 2001); the eolian deposits in north China suggest that the winter monsoon became incrementally strong during the Pleistocene (Sun et al. 2010), and the uplift of mountains in Honshu, Japan, started in the late Pliocene (Yonekura et al. 2001).

*Daphniphyllum*, the sole genus of Daphniphyllaceae, is the evergreen broad-leaved woody plant, and most of the 16 species

are distributed in East and Southeast Asia, the Indian Subcontinent, and Australasia (Huang 1996; Tang et al. 2012). *Daphniphyllum macropodium* Miq. is distributed in southeast China, Taiwan, South Korea, and Japan. In Japan, the tree variety, *D. macropodium* var. *macropodium*, exceeding 10 m in height, is distributed in a warm temperate climate with light snowfall along the Pacific Ocean of Honshu, Shikoku, Kyushu, and the Ryukyu Islands. In addition, a shrub variety, *D. macropodium* var. *humile* (Maxim. ex Franch. et Sav.) K. Rosenthal (syn. *D. humile* Maxim. ex Franch. et Sav.) is distributed in cool temperate climate with heavy snowfall in Hokkaido and along the Sea of Japan of Honshu (Fig. 1). In contrast to the wide distribution of var. *macropodium* across East Asia, var. *humile* is endemic in Japan. The distribution of var. *humile* is concordant with the range of heavy snowfall over 50 cm (Fig. 1) and the duration of snow cover of around 30–120 days (Roessler and Dietz 2022). In contrast to the tree form of var.

**Table 1.** Sampling locality and genetic diversity estimates within populations collected from Japan and South Korea.

TAXON	GROUP	POP CODE	ISLAND	LATITUDE	LONGITUDE	TREE HEIGHT (m)	SNOW DEPTH (m)	ALTITUDE (m)	N	S	H <sub>E</sub>	F <sub>IS</sub>
<i>D. macropodum</i> var. <i>macropodum</i>												
	M	M1	Honshu	37.175	140.990	<10	0.08	1000	4	675	0.09	0.12
		M2	Honshu	36.225	140.107	<15	0.06	300	4	850	0.11	0.07
		M3	Honshu	35.177	140.096	<15	0.05	300	4	1107	0.14	0.07
		M4	Kouzu	34.219	139.159	<5	0.00	400	3	941	0.12	0.03
		M5	Honshu	34.880	138.908	<15	0.13	400	3	1045	0.13	0.06
		M6	Honshu	34.984	137.582	<15	0.04	600	4	1189	0.15	0.12
		M7	Honshu	35.563	136.929	<10	0.41	200	3	679	0.09	0.04
		M8	Honshu	34.139	136.165	<15	0.00	200	4	1121	0.14	0.10
		M9	Honshu	35.063	134.659	<10	0.00	500	3	763	0.11	0.10
		M10	Honshu	34.483	132.312	<15	0.50	600	4	831	0.11	0.10
		M11	Shikoku	33.716	133.608	<10	0.00	700	4	1166	0.14	0.06
		M12	Shikoku	32.863	132.851	<10	0.00	700	3	1229	0.15	0.03
		M13	Kyushu	32.753	131.530	<15	0.00	900	3	1188	0.15	0.06
		M14	Kyushu	32.056	131.198	<15	0.00	200	4	1328	0.16	0.09
		M15	Yaku	30.303	130.552	<15	0.00	1200	4	1114	0.14	0.10
		M16	Jeju	33.321	126.606	<10	—	400	4	1283	0.16	0.08
<i>D. macropodum</i> var. <i>humile</i>												
	HN	H1	Hokkaido	44.775	142.248	<0.5	1.72	100	4	926	0.12	0.08
		H2	Hokkaido	44.107	145.093	<1	1.37	300	4	644	0.09	0.08
		H3	Hokkaido	43.298	142.459	<0.5	0.74	400	4	918	0.12	0.09
		H4	Hokkaido	42.103	143.042	<0.5	0.55	100	4	817	0.10	0.07
		H5	Hokkaido	43.059	141.517	<0.5	1.09	30	4	886	0.11	0.05
		H6	Hokkaido	41.786	141.016	<0.5	0.99	200	4	910	0.11	0.09
		H7	Honshu	40.417	140.207	<0.5	1.84	600	4	958	0.12	0.10
		H8	Honshu	39.869	140.929	<0.5	1.25	900	4	1107	0.14	0.10
		H9	Honshu	39.184	140.947	<0.5	1.23	600	4	1293	0.15	0.05
		H10	Honshu	39.159	140.019	<0.5	2.95	600	4	1201	0.15	0.11
	HS	H11	Honshu	38.236	140.254	<0.5	0.49	300	4	1411	0.17	0.05
		H12	Honshu	37.624	139.537	<0.5	1.09	400	4	1441	0.17	0.06
		H13	Sado	38.227	138.406	<2	0.30	200	4	1375	0.17	0.08
		H14	Honshu	37.036	139.373	<1	2.21	1600	4	1399	0.17	0.06
		H15	Honshu	36.954	138.710	<1	2.31	700	4	1347	0.16	0.06
		H16	Honshu	36.740	137.811	<0.5	1.72	1100	3	1262	0.16	0.04
		H17	Honshu	36.345	137.486	<0.5	1.27	1600	4	1214	0.14	0.06
		H18	Honshu	36.202	136.388	<5	0.91	300	6	1606	0.18	0.09
		H19	Honshu	35.535	136.225	<5	0.61	400	6	1716	0.19	0.07
		H20	Honshu	35.334	135.792	<2	1.35	600	4	1487	0.17	0.03
		H21	Honshu	35.358	134.507	<0.5	2.27	1300	4	1283	0.15	0.05
		H22	Honshu	35.387	133.532	<1	1.43	900	4	1217	0.15	0.08
		H23	Honshu	34.697	132.188	<1	1.21	900	5	1423	0.16	0.09
<i>D. teijemannii</i>												
	Boso Peninsula	Honshu	35.172	140.099	<15	0.05	200	4	—	—	—	—
	Izu Peninsula	Honshu	34.872	139.116	<20	0.03	50	3	—	—	—	—
	Yaku Island	Yaku	30.363	130.657	<20	0.00	100	4	—	—	—	—

Pop code population code, Tree height approximate maximum tree height of population, Snow depth maximum snow depth of population location, N number of individuals used in RAD-seq analysis, S number of segregating sites, H<sub>E</sub> expected heterozygosity, F<sub>IS</sub> fixation index.

*macropodum* with a single straight trunk owing to apical dominance, var. *humile* grows horizontally owing to lateral dominance and clonal reproduction by layering due to being pressed to the ground by snow weight. In addition, short individuals of var. *humile* with a diameter below 1 cm at ground height can bloom (Yoichi, field observations), indicating that the reproductive size of var. *humile* is notably shorter than that of var. *macropodum*. Because individuals of the two varieties experimentally planted at the same place in the Pacific Ocean side of Honshu (35.7753N, 139.9023E) exhibited tree and shrub, respectively (Yoichi, field observations), it suggests that this tree form variation of the two varieties can be determined genetically. Such wide tree height variation is notable between shrubs and these congeners in Japan. The two varieties do not show differences in flower morphology; therefore, we adopt taxonomic treatment as two varieties. Pollination of *D. macropodum* occurs via wind (Kato 2000), and seed dispersal occurs via birds (Kominami et al. 1997).

In the present study, we performed a population genetic analysis of the two *D. macropodum* varieties, with *D. teijsmannii* as an outgroup, using chloroplast DNA (cpDNA) sequences and double digest restriction-site associated DNA (ddRAD) sequencing. To elucidate the evolutionary process of the shrub variety, which is considered related to the development in the heavy snowfall climate, we aimed to: (i) reveal genome-wide divergence between the two varieties, (ii) elucidate relationships between genetic and climatic differentiations between the two varieties, and (iii) discuss whether the evolution of var. *humile* is associated with the development of snowfall along the Sea of Japan during the Quaternary. Our results will provide new knowledge regarding the evolutionary process with ecological specialization and help us to understand tree form evolution and its genetic mechanisms.

## MATERIALS AND METHODS

### Plant sampling

We collected leaf materials from mature individuals from 16 populations of *D. macropodum* var. *macropodum* from Japan and South Korea and 23 of *D. macropodum* var. *humile* from Japan for covering the entire range (Table 1 and Fig. 1). The varieties of populations were identified based on measurements of the maximum tree height of each population because there were mature and immature individuals with various ages. In addition, we sampled three populations of *D. teijsmannii*, which is the other species of the genus distributed in Japan and South Korea, as an outgroup. The collected leaf tissues were immediately dried using silica gel.

### DNA experiment

Genomic DNA was extracted from dried leaves using a modified cetyltrimethylammonium bromide method (Murray and Thompson 1980) after treatment with sorbitol buffer (Wagner et al. 1987). On the basis of a screening of polymorphic loci using previously reported universal primers (Kress et al. 2005; Shaw et al. 2005), three noncoding cpDNA regions [*trnK-matK*, *trnD-trnE*, and *psbH-psbB* (Shaw et al. 2005)], which were polymorphic within and between *D. macropodum* and *D. teijsmannii*, were used in this study. Four individuals from each population of *D. macropodum* and two individuals from each population of *D. teijsmannii* were amplified and sequenced using the protocols described in Yoichi et al. (2017). Genome-wide single-nucleotide polymorphisms (SNPs) were detected using the ddRAD sequencing method, as described in Yoichi et al. (2019). Briefly, the genomic DNA of each sample was digested with *Bg*II and *Eco*RI, and digested fragments of 350–400 bp were sequenced with 150 bp paired-end reads using a HiSeqX platform (Illumina, San Diego, California, USA). Raw reads were processed using fastp v.0.20.1 (Chen et al. 2018) to cut adaptor sequences and filter out sequences with a Phred quality score,  $Q < 30$ .

### SNP detection

Before SNP calling, samples with less than 150 K single-end reads were removed; therefore, 165 samples (an average of 3.9 samples per population) were used for SNP detection. SNPs from single-end reads were called using Stacks v. 2.3 (Catchen et al. 2013). To create stacks, we used the following settings with the outgroup species: minimum depth option for creating a

stack, -m 3; maximum distance between stacks within an individual, -M 3; number of mismatches between loci, -n 2; gapped option for creating stacks, -max\_gaps 5; and default settings for other options. To maximize the number of used SNPs in each data analysis, we defined and made the following three types of datasets that were tailored to the objective of each analysis: 42 populations of *D. macropodum* and *D. teijsmannii* for analyses with the outgroup (Set 1), 39 populations of *D. macropodum* for population genetic analyses of the species (Set 2), and 3 groups of *D. macropodum* for demographic analysis of the species (Set 3). The definitions of the three groups, var. *macropodum* (M) and southern and northern var. *humile* (HS and HN), were populations M1–M16, H11–H23, and H1–H10, respectively, which were identified by population genetic analyses (see Results). For Set 1 and Set 2, we extracted SNPs under Hardy–Weinberg equilibrium, with independent loci, removing minor alleles and allowing missing sites, by applying the following restrictions using the Populations program in Stacks: minimum minor allele frequency was 1%, -min\_maf 0.01; observed heterozygosity less than 0.5, -max\_obs\_het 0.5; genotyping rate more than 20% of individuals within populations, -r 0.2; and present in all of the populations, -p 42 or 39. Pairwise  $R^2$  values for each SNP pair were calculated using PLINK 1.90b (Purcell et al. 2007), and loci with values higher than 0.8 were removed using the whitelist option in the populations to exclude SNPs with high linkage equilibrium. SNP genotypes for the three groups in *D. macropodum* (Set 3) were called with the following restrictions: include all SNPs without minor allele filter, -min\_maf 0.00; observed heterozygosity less than 0.5, -max\_obs\_het 0.5; genotyping rate more than 80% of individuals within regions, -r 0.8; and present in all of the regions, -p 3.

### Population genetic analysis

cpDNA sequences were edited and assembled using DNA Baser 4 (Heracle BioSoft, Pitești, Romania) and aligned using MUSCLE implemented in MEGA 5 (Edgar 2004; Tamura et al. 2011). A haplotype network was constructed by the median-joining method using NETWORK v. 10 (Fluxus Technology Ltd, Colchester, UK).

Genetic relationships among populations, with and without the outgroup species, were constructed independently by the neighbor-joining method based on  $D_A$  distances (Nei et al. 1983) using POPTREE2 (Takezaki et al. 2010). The significance of nodes was evaluated from bootstrap values based on 1000 replicates. The individual-based genetic structure with and without the outgroup species was inferred independently by the sparse non-negative matrix factorization method using sNMF (Frichot et al. 2014). Different numbers of ancestries ( $K$ ) in the 1–10 range were tested and ranked using the cross-entropy criterion. Principal component analysis (PCA) of individuals was performed using the R package adegenet of R v. 4.1.1 (Dray and Dufour 2007).

### Demographic analysis

To estimate past population demography, such as population size change, population divergence, or migration between populations, approximate Bayesian computation (ABC) was performed. On the basis of the results of population genetic analyses (see Results), we classified populations into three different groups: var. *macropodum* (M, populations M1–M16), southern var. *humile* (HS, populations H11–23), and northern var. *humile* (HN, populations H1–H10). We then created four three-population divergence scenarios: no migration (NM), isolation with migration (IM), ancient migration (AM), and secondary contact (SC) (Fig. 2). NM assumes no migration between the populations. IM assumes that migration between populations always occurs from its divergence to the current. AM assumes that migration occurred only in the early period of its divergence. SC assumes that migration occurs after a certain period of isolation. First, we tested two migration patterns, the island and stepping-stone models, for IM from  $T_0$  to  $T_2$  and SC from  $T_0$  to  $T_1$ . The island model assumes that migration occurs between all pairs of groups. The stepping-stone model assumes that migration occurs only between adjacent pairs of groups. In our preliminary analyses, as the stepping-stone model was more strongly supported than the island model in both IM and SC (details not shown), we used the stepping-stone model for IM and SC in the scenario comparison. Prior distributions of the effective population size ( $N$ ), time ( $T$ ), and migration ( $Nm_{ij}$ ) parameters were log-uniform ( $10^3$ ,  $10^6$ ), log-uniform (1,  $10^6$ ), and log-uniform (0.1, 10), respectively (Supplementary Table 1). The units were the number of diploid individuals generations ago and the number of migrants per generation from  $j$  to  $i$ , respectively. To aid the reader's understanding, the direction of migration is shown as the movement of individuals from  $j$  to  $i$  (time in forward).

We calculated two-dimensional minor allele site frequency spectra (2D-minor allele SFSs) between two group pairs using our own R scripts using the

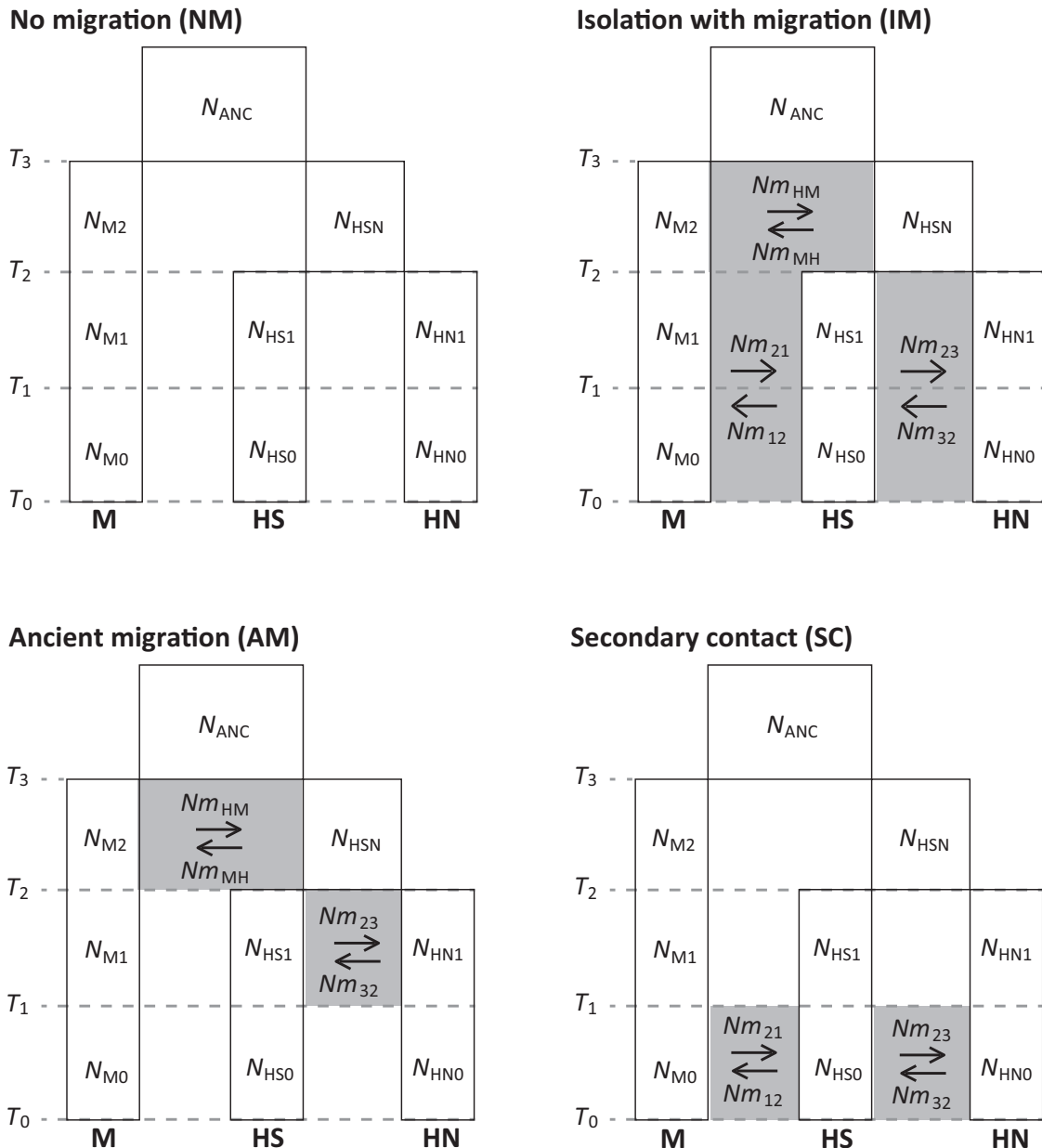


**Fig. 2 Comparison of the three group divergence scenarios.** The four scenarios are no migration (NM), isolation with migration (IM), ancient migration (AM), and secondary contact (SC). M, *Daphniphyllum macropodum* var. *macropodum*; HS and HN, southern and northern *D. macropodum* var. *humile*, respectively. N, effective population size; T, event time;  $Nm_{ij}$ , number of migrants per generation from j to i (1, M; 2, HS; 3 HN). Direction of migration is forward in time. The period shown in light gray indicates that a migration is occurring.

dataset for ABC analyses (Set 3). Missing data were compensated for by bootstrapping within a group. We then calculated the number of polymorphic sites ( $S$ ), nucleotide diversity ( $\pi$ ), and Tajima's  $D$  ( $D$ ) for each group, and  $F_{ST}$  between group pairs (Wright 1951) from 2D-minor allele SFSs. The four scenarios were simulated  $10^4$  times each with fastsimcoal2 v. 2705, which enables us to analyze geographically structured populations (Excoffier et al. 2021). The 12 summary statistics were calculated from the output 2D-minor allele SFSs. To simulate the data as realistically as possible, the same number of short leads (2279 loci) and average length (151.21 bp) as the observed data were used. The mutation rate estimated in the woody species *Populus tremula* ( $1.74 \times 10^{-8}$  per site per generation) was used (Gossmann et al. 2012). Because we simulated very short DNA sequences, the recombination rate was set to 0. Simulated scenarios were compared using ABC-random forest (RF) implemented in the abcrf package of R v. 1.8.1 with 1000 decision trees (Pudlo et al. 2016). The confusion matrix of the scenarios, classification error rates, and posterior probability were calculated. Using the best scenario selected by ABC-RF, an additional  $4 \times 10^6$

simulations were performed for parameter estimation. With the 1000 simulations closest to the observed data, posterior distributions of the parameters were estimated by a neural net regression method implemented in the abc package of R v. 2.1 (Blum and François 2010; Csilléry et al. 2012). The number of neural networks was set to 20. The logit transformation of the parameters was used to maintain the estimated value within the prior range. The posterior mode was estimated by the density function of R. The 95% highest posterior density (HPD) was estimated using the coda package of R v. 0.19.4 (Plummer et al. 2006). Event times were converted from generations ago to years ago using the value of 20 years per generation, which was determined by considering the species life history, although the two varieties have different life forms associated with different maturation times (Petit and Hampe 2006).

To confirm the fit of the scenario to the observed data, posterior predictive simulation with 1000 randomly drawn posterior samples was conducted, and summary statistics were compared to the observed data (Gelman et al. 2014).

## Climatic differentiation

To evaluate the differentiation of habitats, the maximum snow depth at 30 arc-sec resolution from the Japan Meteorological Agency (<https://www.data.jma.go.jp/obd/stats/etn/view/atlas.html>) was obtained, and the values of the analyzed populations were retrieved. Because it is difficult to identify the difference in tree height between the two varieties from herbarium specimens, we used only the locality of the analyzed populations for evaluating climatic differentiation. We applied analysis of variance with Tukey's multiple comparisons of means, using R v.3.5.2, to determine whether snow depth differed among the three groups. Because of a lack of a value of the maximum snow depth from Jeju Island in South Korea, this population was removed from this analysis.

## RESULTS

### Distribution of chloroplast DNA haplotypes for the two species

The sequences of three cpDNA regions were obtained from 64 individuals of *Daphniphyllum macropodum* var. *macropodum*, 92 of *D. macropodum* var. *humile*, and 11 of *D. teijsmannii*. The lengths of the aligned sequences for the three regions were 739 bp for *trnK-matK*, 545 bp for *trnD-trnE*, and 560 bp for *psbH-psbB*. These sequences identified four haplotypes from four segregating sites across the two species. A haplotype network revealed that the haplotypes could be distinguished with one or two substitution steps. *Daphniphyllum macropodum* var. *macropodum* had two haplotypes (1 and 2) and var. *humile* had two haplotypes (2 and 3); thus, haplotype 2 was shared between the two varieties in western Japan (Fig. 1a).

### Phylogeographic patterns of SNPs for the two species and two varieties

The RAD-seq library yielded 368,840,797 single-end reads with an average of 3,226,768 per sample. We detected 2194 SNPs with a genotyping rate of 85.15% with the outgroup (Set 1) and 3053 SNPs with a genotyping rate of 82.44% without the outgroup (Set 2). The number of polymorphic SNPs and expected heterozygosity within each population of *D. macropodum* (Set 2) ranged from 644 to 1716 and 0.085 to 0.187, respectively (Table 1). Genetic relationships among populations by the neighbor-joining method revealed that *D. teijsmannii* and the two varieties of *D. macropodum* were distinguished with the highest probability (100%), and the two varieties were distinguished in both the SNP sets with and without the outgroup (Fig. 3). Furthermore, genetic relationships among populations identified two groups, populations H1–H10 and H11–H23, within var. *humile* with the highest probability (Fig. 3b). The individual-based genetic structure with the outgroup, inferred by sNMF, showed that the optimal number of clusters ( $K$ ) was  $K = 4$ , based on the cross-entropy criterion. For all  $K = 2$ – $5$ , *D. macropodum* and *D. teijsmannii* were clearly distinguished by different clusters (Supplementary Fig. 1). The individual-based genetic structure without the outgroup showed that the optimal number of clusters was  $K = 4$ . For all  $K = 2$ – $5$ , clusters were admixed between the two varieties (Fig. 1d), and this pattern was the same when including the outgroup. PCA showed that the first component (85.1%) had a high contribution to the variance explained. Three groups, that is, var. *macropodum* (M, populations M1–M16), southern var. *humile* (HS, populations H11–23), and northern var. *humile* (HN, populations H1–H10), could be clearly identified by the first two PCA axes (Fig. 4).

### Demographic analysis

We detected 5858 SNPs with a genotyping rate of 91.58% for the demographic analysis dataset (Set 3). Pairwise genetic differentiation ( $F_{ST}$ ) between groups was highest between M and HN (0.071) and lowest between M and HS (0.022; Supplementary Fig. 2). The isolation with migration (IM) was selected as the best scenario by ABC-RF with a high posterior probability of 0.808 (Table 2). Although the classification error rate was relatively high (0.501) as

votes by an RF were concentrated into the IM (0.844), the posterior probability of the best scenario was high (0.808) and the error rate when the IM was the true scenario was moderate (0.328; Supplementary Table 2). Therefore, we confirmed that our ABC-RF scenario choice was reliable. All posterior distributions of parameters in the IM showed a different shape from their prior distributions and showed a clear peak (Supplementary Fig. 3). Posterior predictive simulation of the IM showed that all simulated parameters were located around the observed value (Supplementary Fig. 2). This indicates that the goodness-of-fit of the IM is high.

The posterior modes (95% HPDs) of the effective population sizes at present of M, HS and HN were 62,538 (2399–976,341), 2649 (1014–594,108) and 28,699 (2223–873,117), respectively (Fig. 5 and Supplementary Table 3). Posterior distributions of the ratio of effective population size at present to that at  $T_1$  ( $N_0/N_1$ ) in M and HN were biased to larger than 1.0 (0.0 on the log-scale) with posterior probabilities ( $N_0 > N_1$ ) 0.665 and 0.744, respectively (Supplementary Fig. 4c). However, that in HS was distributed around 1.0. This indicated that M and HN expanded in size from  $T_1$  to the present, whereas HS did not. Although we also examined population size changes from  $T_1$  to  $T_2$  and  $T_2$  to  $T_3$ , there were no clear expansion or reduction signals in population size (Supplementary Fig. 4a, b). The posterior modes (95% HPDs) of  $T_1$ ,  $T_2$  and  $T_3$  were 20 (0–393), 198 (14–4464), and 1316 (282–19,984) Kya, respectively. Migration was more frequent from the present to  $T_2$  than from  $T_2$  to  $T_3$  (Fig. 5 and Supplementary Table 3). Especially in the direction toward HS, the values of the number of migrants per generation ( $Nm$ ) were larger than those of the others [from M, 4.24 (0.68–9.66); from HN, 3.29 (0.36–8.18)].

### Tree height variation and habitat differentiation

The approximate maximum tree height of the population for M, HS and HN ranged from 5 to 15 m, 0.5 to 1 m, and 0.5 to 5 m, respectively (Table 1 and Fig. 1c). The maximum snow depth of the analyzed population of var. *humile* ranged from 0.30 to 2.95 m (Table 1). The approximate maximum tree height and maximum snow depth of the population significantly differed between groups of M and HN, and M and HS ( $P < 0.001$ ), but not between HN and HS, respectively.

## DISCUSSION

### Genetic relationships of *Daphniphyllum* species in Japan and South Korea

When considering evolution and population genetic structure, introgression can have non-negligible effects on evolution and species relationships (Barton 2001; Abbott et al. 2013). *Daphniphyllum* species, distributed in Japan and South Korea, consist of only *D. macropodum* and *D. teijsmannii*. The genetic divergence of the two species, which are rarely found in the same area, is clear, suggesting that the influence of introgression on the two species, especially in *D. macropodum*, is negligible in this study (Fig. 3a).

### Genetic differentiation between the two varieties of *D. macropodum*

*Daphniphyllum macropodum* var. *macropodum* and var. *humile* have also diverged with the highest support (Fig. 3). It suggests that the morphological difference between the two varieties, which are characterized by tree height, may be environmentally controlled and also genetically predetermined. In Japan, plant distributions have changed during climatic oscillations of the late Quaternary and such history is reflected in genetic structure. However, widespread trees without morphological differences between heavy and light snowfall climates exhibit weak genetic structures corresponding to snowfall in western Honshu (Sakaguchi et al. 2011; Iwasaki et al. 2012), while the genetic structure of the two varieties seems to maintain divergence between the varieties (Fig. 2b). Difference in habitats between the two varieties

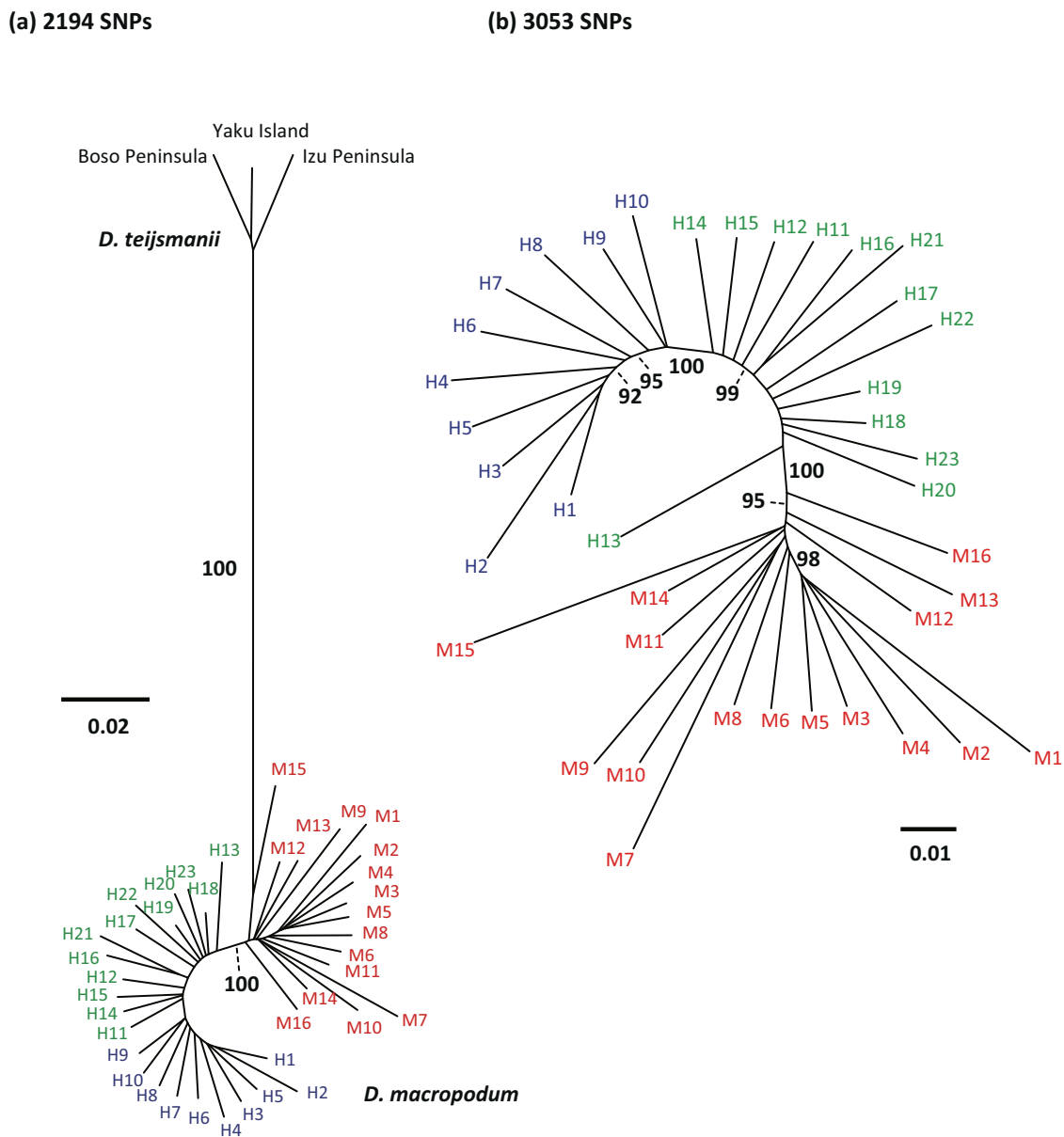


**Fig. 3** Genetic relationships among populations, constructed based on  $D_A$  distance using the neighbor-joining method. Relationships **a** with and **b** without the outgroup species, *Daphniphyllum teijsmannii*. Bootstrap probabilities that were **a** 100% and **b** exceeded 80% based on 1000 replicates are shown above nodes. Populations codes are shown in Table 1. Red, green and blue are *Daphniphyllum macropodum* var. *macropodum* (M), southern (HS) and northern (HN) *D. macropodum* var. *humile*, respectively.

based on climate, including snowfall, suggests that heavy snowfall is considered to be a significant selective pressure for var. *humile* to maintain the shrub form as same as other shrubs (Kume et al. 1998).

The distribution of plants with morphological differences, that is, distribution in a light snowfall region along the Pacific Ocean and the heavy snowfall region along the Sea of Japan in the Japanese archipelago, is known for many species. Ecological and morphological differences, such as leaf size, leaf shape, snow weight tolerance, and a loss of drought tolerance, between regions are considered to be a result of adaptations to heavy snowfall climate (Hagiwara 1977; Kume and Ino 2000; Tamaki et al. 2018). As a result, a deciduous broad-leaved tree, *Magnolia salicifolia* exhibited that morphological and genetic differentiations were associated (Tamaki et al. 2018). The evergreen broad-leaved shrub, *Aucuba japonica* var. *borealis*, which has morphological features similar to those of *D. macropodum* var. *humile* in

the heavy snowfall region (Kume and Ino 2000), also exhibited that morphological and genetic differentiations were not associated with geographic distribution in diploid and tetraploid individuals (Ohi et al. 2003). Furthermore, *Fagus crenata* (Hiraoka and Tomaru 2009) and an evergreen conifer, *Cryptomeria japonica* (Kimura et al. 2014), which have morphological differences between heavy and light snowfall climates, exhibited genetic divergences between populations in the Pacific Ocean and the Sea of Japan sides but admixed population genetic structures, which may suggest the presence of migration between the regions. These evidence indicate that the evolution in the heavy snowfall region and the maintenance of genetic differentiation vary within the same landscape.

In contrast to the genetic divergence of the two varieties, genetic differentiation between var. *macropodum* (M) and the southern group of var. *humile* (HS;  $F_{ST} = 0.022$ ) was lower than that between the two groups of var. *humile* ( $F_{ST} = 0.053$ ;

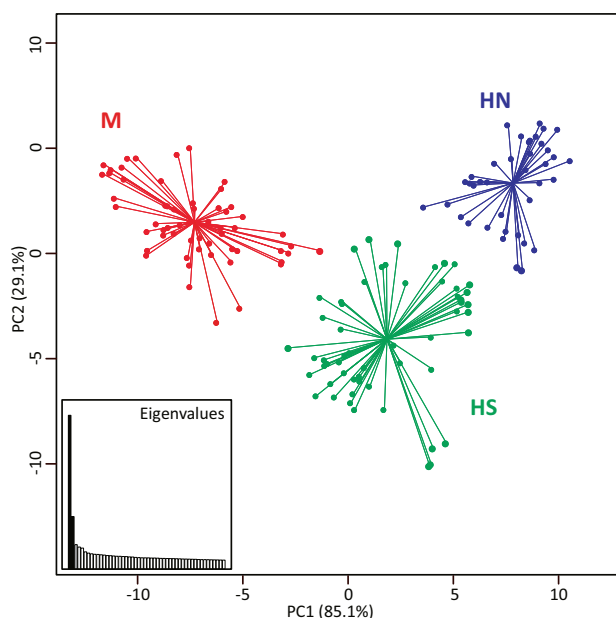


**Fig. 4 Genetic relationships among individuals detected by principal component analysis (PCA).** M, *Daphniphyllum macropodum* var. *macropodum*; HS and HN, southern and northern *D. macropodum* var. *humile*, respectively. Proportions of variance explained for the two principal components were evaluated from the top 50 components.

Supplementary Fig. 2). These relationships between groups can be explained by the strength of migration between groups, which was larger in M-HS pair than in HS-HN pair (Fig. 5). This result seems to be reliable for considering a tendency that tree height is tall in the northern and short in the southern groups of var. *humile* (Table 1). Especially the existence of taller populations in southern var. *humile* (HS) suggests migration between the two varieties. The migration is also supported by the shared cpDNA haplotype (haplotype 2) of the two varieties in western Honshu (Fig. 1a), and it indicates that migration occurs not only by pollen flow via wind but also by seed dispersal via birds (Kominami et al. 1997; Kato 2000). In addition, migration seems to be predominant from var. *macropodum* into southern var. *humile*, as shown in the demographic analysis (Fig. 5). In contrast, the unshared haplotype (haplotype 1) of the two varieties in eastern Honshu suggests that the distribution of southern var. *humile* may be formed by range expansion from the south. Demographic analyses using user-friendly programs such as DIY-ABC enable the modeling of admixture at a timepoint but cannot consider continuous

**Table 2.** Summary table of ABC-RF scenario choices.

Votes by random-forests				Posterior probability	Error rate
NM	IM	AM	SC		
0.006	<b>0.844</b>	0.051	0.099	0.808	0.501

NM no migration, IM isolation with migration, AM ancestral migration, SC secondary contact.

The bold font indicates the best scenario.

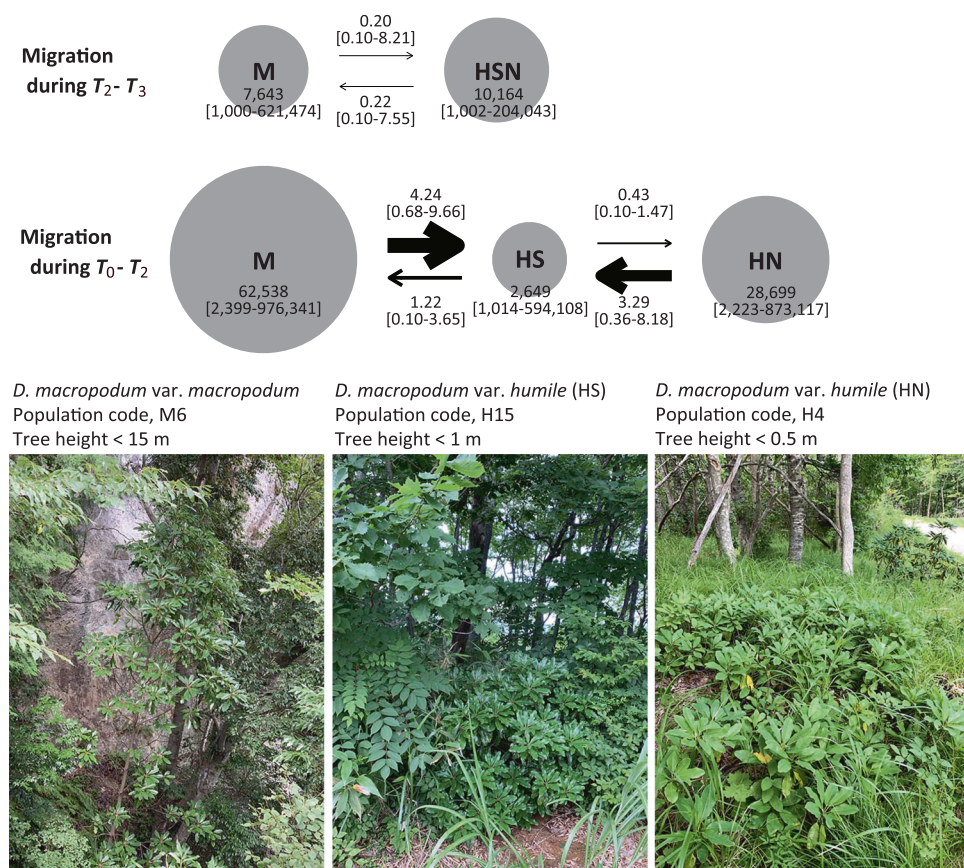


**Fig. 5 The effective population size and number of migrants per generation in the three island groups are denoted by circles and arrows, respectively, in the best scenario (isolation with migration, IM).** The sizes of the circles and arrows are proportional to the value of the posterior mode of the parameter. The effective population sizes were at  $T_2$  and  $T_0$ . Numbers indicate posterior mode with 95% highest posterior density. Direction of migration is forward in time. Photographs were obtained for each representative population. M, *Daphniphyllum macropodum* var. *macropodum*; HS and HN, southern and northern *D. macropodum* var. *humile*, respectively.

migrations in scenarios (Cornuet et al. 2014). Our demographic analysis using isolation with migrations is considered to reflect more actual demography of migration. It may be difficult to evaluate whether the definition of groups, based on the among-population relationships and individual relationships (Figs. 3 and 4), represents the actual population dynamics because of the gradual population genetic structure in var. *humile* (Fig. 1d).

The short tree height of var. *humile* is considered an adaptive trait against cold climate by being buried in snow cover (Kume and Ino 1993); therefore, short tree height would be essential for survival in a heavy snowfall climate. Another shrub species *Camellia rusticana*, which is endemic in the heavy snowfall region, and *C. japonica* in the light snowfall region have different physiological tolerance to heavy snowfall climate (Kume et al. 1998); therefore, the shrub variety of *Daphniphyllum* may also evolve such physiological tolerance (Katahata et al. 2014). In var. *humile*, some populations in western Honshu tend to be taller than northern populations (Table 1); thus, tall populations in this region may indicate that the snow cover in these populations is sufficient to bury individuals or temperatures not low enough to damage leaves (Kume and Ino 1993). Furthermore, in southern var. *humile*, mixing proportions of the genetic clusters, which dominated in the two varieties (Fig. 1b), in addition, tree heights tended to be variable among populations, especially in western Honshu (H18–H23; Table 1). These lines of evidence suggest that the tree height variation with migration is considered to be maintained by both the geographic proximity of the two varieties and climatic selection in habitats. However, the approximate maximum tree height described in this study is insufficient and should be improved by measuring the maximum and minimum range of tree height of mature individuals with sex in populations.

### The timing of adaptation of *D. macropodum* var. *humile* to heavy snowfall environment

On the basis of a phylogenetic analysis of *Daphniphyllum* (Tang et al. 2022), vars. *macropodum* and *humile* were closely related within the genus, and other closely related species to var. *humile* are also taller than the shrub variety. In addition, the distribution of var. *macropodum* is wide across southeast China, Taiwan, South Korea, and Japan (Tang et al. 2012). These pieces of evidence support the hypothesis that the shrub variety evolved from the tree variety. However, the shrub variety of evergreen conifer *Torreya nucifera* var. *radicans*, in the heavy snowfall region was not the most closely related to the tree variety *Torreya nucifera* var. *nucifera* in the light snowfall region of Japan (Aizawa and Worth 2021). Therefore, more reliable phylogenetic trees of *Daphniphyllum* will help us to understand the evolutionary history of var. *humile*. The IM scenario in this study was robust, whereas the divergence time of the two varieties was controversial because it is highly dependent on the applied mutation rate and generation time. In this simulation, the divergence time of the two varieties was estimated to be 1316 Kya (282–19,984, 95% HPD). Global cooling since the mid-Miocene and climatic oscillations since the Pleistocene (Zachos et al. 2001) influenced snowfall in Japan, the eolian deposits in north China suggest that the winter monsoon became incrementally stronger during the Pleistocene (Sun et al. 2010), and the uplift of mountains in Honshu has been activated since the late Pliocene (Yonekura et al. 2001). In addition, discoveries of *Stewartia monadelpha* fossils, which is currently growing in light snowfall region of the Pacific Ocean side of Japan, a living fossil conifer, *Metasequoia glyptostroboides*, from layers during 1.5–1.8 Mya in central Niigata (37.40–37.80N, 148.46–148.50S) along the Sea of Japan, which is currently a heavy snowfall area (Momohara et al. 2017), and an increase of *Cryptomeria japonica* pollen from sediments from Sea of Japan off at 2.5 and 1.7 Mya (Igarashi et al. 2018) suggests that this area had become cold and started to experience heavy snow since the period. Therefore, the divergence of the two varieties and range expansion of var. *humile* might have occurred since the Middle Quaternary.

### CONCLUSION

The short tree height of var. *humile* is considered to be an adaptive trait to the heavy snowfall climate. The migration between the shrub and tree varieties since the divergence suggests that selective pressure by snow cover and cold hardiness is geographically shifted. This provides important knowledge for studies on ecological speciation with migration and on evolution associated with adaptation to climate, which is sometimes gradually changing. The evolution of the shrub variety could be associated with a lack of apical dominance, and thinness and plasticity of stems, resource allocation, and reproductive size.

### DATA AVAILABILITY

Genotype data of SNPs and the script for demographic analysis used for this study will be available at Dryad: <https://doi.org/10.5061/dryad.70rxwdc3x>.

### REFERENCES

Abbott R, Albach D, Ansell S, Arntzen JW, Baird SJE, Bierne N et al. (2013) Hybridization and speciation. *J Evol Biol* 26:229–246

Aizawa M, Worth JRP (2021) Phylogenetic origin of two Japanese *Torreya* taxa found in two regions with strongly contrasting snow depth. *J Plant Res* 134:907–919

Barton NH (2001) The role of hybridization in evolution. *Mol Ecol* 10:551–568

Blum MGB, François O (2010) Non-linear regression models for Approximate Bayesian Computation. *Stat Comput* 20:63–73

Böhle U-R, Hilger HH, Martin WF (1996) Island colonization and evolution of the insular woody habit in *Echium* L. (Boraginaceae). *Proc Natl Acad Sci USA* 93:11740–11745

Brown JH (1995) *Macroecology*. University of Chicago Press, Chicago, IL

Catchen J, Hohenlohe PA, Bassham S, Amores A, Cresko WA (2013) Stacks: an analysis tool set for population genomics. *Mol Ecol* 22:3124–3140

Chen S, Zhou Y, Chen Y, Gu J (2018) fastp: an ultra-fast all-in-one FASTQ preprocessor. *Bioinformatics* 34:i884–i890

Cornuet JM, Pudlo P, Veyssié J, Dehne-Garcia A, Gautier M, Leblois R et al. (2014) DIYABC v2.0: a software to make approximate Bayesian computation inferences about population history using single nucleotide polymorphism, DNA sequence and microsatellite data. *Bioinformatics* 30:1187–1189

Csillér K, François O, Blum MGB (2012) abc: an R package for approximate Bayesian computation (ABC). *Methods Ecol Evol* 3:475–479

Dray S, Dufour AB (2007) The ade4 package: implementing the duality diagram for ecologists. *J Stat Softw* 22:1–20

Edgar RC (2004) MUSCLE: multiple sequence alignment with high accuracy and high throughput. *Nucleic Acids Res* 32:1792–1797

Excoffier L, Marchi N, Marques DA, Matthey-Doret R, Gouy A, Sousa VC (2021) Fastsimcoal2: demographic inference under complex evolutionary scenarios. *Bioinformatics* 37:4882–4885

Foster SA, McKinnon GE, Steane DA, Potts BM, Vaillancourt RE (2007) Parallel evolution of dwarf ecotypes in the forest tree *Eucalyptus globulus*. *N Phytol* 175:370–380

Fritchot E, Mathieu F, Trouillon T, Bouchard G, François O (2014) Fast and efficient estimation of individual ancestry coefficients. *Genetics* 196:973–983

Futuyma DJ, Moreno G (1988) The evolution of ecological specialization. *Annu Rev Ecol Syst* 6:207–233

Gelman A, Carlin JB, Stern HS, Dunson DB, Vehtari A, Rubin BD (2014) *Bayesian data analysis*, 3rd edn. CRC Press, Boca Raton, FL, USA

Gossmann TI, Keightley PD, Eyre-Walker A (2012) The effect of variation in the effective population size on the rate of adaptive molecular evolution in Eukaryotes. *Genome Biol Evol* 4:658–667

Hagiwara S (1977) Clines on leaf size of beech *Fagus crenata* (in Japanese). *Species Biol Res* 1:39–51

Hara M (2023) Phyogeography and history of Japanese beech forests: recent advances and implications for vegetation ecology. *Ecol Res* 38:218–235

Hiraoka K, Tomaru N (2009) Genetic divergence in nuclear genomes between populations of *Fagus crenata* along the Japan Sea and Pacific sides of Japan. *J Plant Res* 122:269–282

Hoekstra HE, Hirschmann RJ, Bunde RA, Insel PA, Crossland JP (2006) A single amino acid mutation contributes to adaptive beach mouse color pattern. *Science* 313:101–104

Hollender CA, Dardick C (2015) Molecular basis of angiosperm tree architecture. *N Phytol* 206:541–556

Huang TC (1996) Notes on taxonomy and pollen of Malesian *Daphniphyllum* (Daphniphyllaceae). *Blumea* 41:231–244

Hughes C, Eastwood R (2006) Island radiation on a continental scale: exceptional rates of plant diversification after uplift of the Andes. *Proc Natl Acad Sci USA* 103:10334–10339

Igarashi Y, Irino T, Sawada K, Song L, Furota S (2018) Fluctuations in the East Asian monsoon recorded by pollen assemblages in sediments from the Japan Sea off the southwestern coast of Hokkaido, Japan, from 4.3 Ma to the present. *Glob Planet Change* 163:1–9

Iwasaki T, Aoki K, Seo A, Murakami N (2012) Comparative phylogeography of four component species of deciduous broad-leaved forests in Japan based on chloroplast DNA variation. *J Plant Res* 125:207–221

Katahata SI, Han Q, Naramoto M, Kakubari Y, Mukai Y (2014) Seasonal changes in temperature response of photosynthesis and its contribution to annual carbon gain in *Daphniphyllum humile*, an evergreen understorey shrub. *Plant Biol* 16:345–353

Kato M (2000) Anthophilous insect community and plant-pollinator interactions on Amami Islands in the Ryukyu Archipelago, Japan. *Contrib Biol Kyoto Univ* 29:157–252

Kawase H, Sasai T, Yamazaki T, Ito R, Dairaku K, Sugimoto S et al. (2018) Characteristics of synoptic conditions for heavy snowfall in western to northeastern Japan analyzed by the 5-km regional climate ensemble experiments. *J Meteorol Soc Jpn* 96:161–178

Kimura MK, Uchiyama K, Nakao K, Moriguchi Y, Jose-Maldia LS, Tsumura Y (2014) Evidence for cryptic northern refugia in the last glacial period in *Cryptomeria japonica*. *Ann Bot* 114:1687–1700

King DA (1990) The adaptive significance of tree height. *Am Nat* 135:809–828

Kominami Y, Tanouchi H, Sato T (1997) Spatial pattern of bird-dispersed seed rain of *Daphniphyllum macropodum* in an evergreen broad-leaved forest. *J Sustain* 6:187–201

Kress WJ, Wurdack KJ, Zimmer EA, Weigt LA, Janzen DH (2005) Use of DNA barcodes to identify flowering plants. *Proc Natl Acad Sci USA* 102:8369–8374

Kume A, Ino Y (1993) Comparison of ecophysiological responses to heavy snow in two varieties of *Aucuba japonica* with different areas of distribution. *Ecol Res* 8:111–121

Kume A, Ino Y (2000) Differences in shoot size and allometry between two evergreen broad-leaved shrubs, *Aucuba japonica* varieties in two contrasting snowfall habitats. *J Plant Res* 113:353–363

Kume A, Tanaka C, Matsumoto S, Ino Y (1998) Physiological tolerance of *Camellia rusticana* leaves to heavy snowfall environments: the effects of prolonged snow cover on evergreen leaves. *Ecol Res* 13:117–124

Maekawa F (1949) Makinoesia and its bearing to Oriental Asiatic flora. *J Jpn Bot* 24:91–96

Momohara A, Ueki T, Saito T (2017) Vegetation and climate histories between MIS 63 and 53 in the Early Pleistocene in central Japan based on plant macrofossil evidences. *Quat Int* 455:149–165

Murray M, Thompson W (1980) Rapid isolation of high molecular weight plant DNA. *Nucleic Acids Res* 8:4321–4326

Nei M, Tajima F, Tateno Y (1983) Accuracy of estimated phylogenetic trees from molecular data. *J Mol Evol* 19:153–170

Ohi T, Kajita T, Murata J (2003) Distinct geographic structure as evidenced by chloroplast DNA haplotypes and ploidy level in Japanese *Aucuba* (Aucubaceae). *Am J Bot* 90:1645–1652

Petit RJ, Hampe A (2006) Some evolutionary consequences of being a tree. *Annu Rev Ecol Evol Syst* 37:187–214

Plummer M, Best N, Cowles K, Vines K (2006) CODA: convergence diagnosis and output analysis for MCMC. *R News* 6:1:7–11

Pudlo P, Marin JM, Estoup A, Cornuet JM, Gautier M, Robert CP (2016) Reliable ABC model choice via random forests. *Bioinformatics* 32:859–866

Purcell S, Neale B, Todd-Brown K, Thomas L, Ferreira MAR, Bender D et al. (2007) PLINK: a tool set for whole-genome association and population-based linkage analyses. *Am J Hum Genet* 81:559–575

Roessler S, Dietz AJ (2022) Development of Global Snow Cover—Trends from 23 Years of Global SnowPack. *Earth* 4:1–22

Sakaguchi S, Takeuchi Y, Yamasaki M, Sakurai S, Isagi Y (2011) Lineage admixture during postglacial range expansion is responsible for the increased gene diversity of *Kalopanax septemlobus* in a recently colonised territory. *Heredity* 107:338–348

Sakai A, Larcher W (1987) Frost survival of plants (ecological studies, Vol. 62). Springer-Verlag, Berlin, Germany

Shaw J, Lickey EB, Beck JT, Farmer SB, Liu W, Miller J et al. (2005) The tortoise and the hare II: relative utility of 21 noncoding chloroplast DNA sequences for phylogenetic analysis. *Am J Bot* 92:142–166

Sun Y, An Z, Clemens SC, Bloemendal J, Vandenberghe J (2010) Seven million years of wind and precipitation variability on the Chinese Loess Plateau. *Earth Planet Sci Lett* 297:525–535

Takezaki N, Nei M, Tamura K (2010) POPTREE2: software for constructing population trees from allele frequency data and computing other population statistics with Windows interface. *Mol Biol Evol* 27:747–752

Tamaki I, Kawashima N, Setsuko S, Itaya A, Tomaru N (2018) Morphological and genetic divergence between two lineages of *Magnolia salicifolia* (Magnoliaceae) in Japan. *Biol J Linn Soc* 125:475–490

Tamura K, Peterson D, Peterson N, Stecher G, Nei M, Kumar S (2011) MEGA5: molecular evolutionary genetics analysis using maximum likelihood, evolutionary distance, and maximum parsimony methods. *Mol Biol Evol* 28:2731–2739

Tang MS, Tsai CC, Yang YP, Sheue CR, Liu SH (2022) A Multilocus Phylogeny of *Daphniphyllum* (Daphniphyllaceae). *Ann Mo Bot Gard* 107:137–152

Tang MS, Yang YP, Tsai CC, Sheue CR (2012) The diversity of pistillate flowers and its taxonomic value to the classification of *Daphniphyllum* (Daphniphyllaceae). *Bot Stud* 53:509–524

Wagner DB, Furnier GR, Saghai-Marsoof MA, Williams SM, Dancik BP, Allard RW (1987) Chloroplast DNA polymorphisms in lodgepole and jack pines and their hybrids. *Proc Natl Acad Sci USA* 84:2097–2100

Wagner ND, Gramlich S, Hörandl E (2018) RAD sequencing resolved phylogenetic relationships in European shrub willows (*Salix* L. subg. *Chamaetia* and subg. *Vetrix*) and revealed multiple evolution of dwarf shrubs. *Ecol Evol* 8:8243–8255

Wright S (1951) The genetical structure of populations. *Ann Eugen* 15:323–354

Yoichi W, Jin XF, Peng CI, Tamaki I, Tomaru N (2017) Contrasting diversification history between insular and continental species of three-leaved azaleas (*Rhododendron* sect. *Brachycalyx*) in East Asia. *J Biogeogr* 44:1065–1076

Yoichi W, Minamitani T, Oh S-H, Nagano AJ, Abe H, Yukawa T (2019) New taxa of *Rhododendron tschonoskii* alliance (Ericaceae) from East Asia. *PhytoKeys* 134:97–114

Yonekura N, Kaizuka S, Nogami M, Chinzei K (2001) Introduction to Japanese geomorphology, 2nd edn. University of Tokyo Press, Tokyo, Japan

Zachos J, Pagani H, Sloan L, Thomas E, Billups K (2001) Trends, rhythms, and aberrations in global climate 65 Ma to present. *Science* 292:686–693

## ACKNOWLEDGEMENTS

We are grateful to Harue Abe, Ryosuke Adachi, Hiroya Hatakawa, Arata Momohara, Hisa Saito, Shota Sakaguchi, Shogo Sugiura, Yuta Takano, Azumi Yano, the University of Tokyo Hokkaido Forest and Hokkaido University Nakagawa Experimental Forest for their help in collecting plant materials. This research was supported by a Grant-in-Aid for Scientific Research (18H02230 and 20H03020) for the Japan Society for the Promotion of Science, KAKENHI.

## AUTHOR CONTRIBUTIONS

WY designed the study. Sample collection was performed by WY, SM, IT and S-HO. The molecular experiments were conducted by WY, SM and AJN. Data were generated, analyzed, and visualized by WY, SM and IT. Manuscript was written by WY, with contributions from all authors.

## COMPETING INTERESTS

The authors declare no competing interests.

## ADDITIONAL INFORMATION

**Supplementary information** The online version contains supplementary material available at <https://doi.org/10.1038/s41437-023-00637-2>.

**Correspondence** and requests for materials should be addressed to Watanabe Yoichi.

**Reprints and permission information** is available at <http://www.nature.com/reprints>

**Publisher's note** Springer Nature remains neutral with regard to jurisdictional claims in published maps and institutional affiliations.

Springer Nature or its licensor (e.g. a society or other partner) holds exclusive rights to this article under a publishing agreement with the author(s) or other rightsholder(s); author self-archiving of the accepted manuscript version of this article is solely governed by the terms of such publishing agreement and applicable law.